

Non-thermal cytocidal effect of infrared irradiation on cultured cancer cells using specialized device

Yohei Tanaka,^{1,3} Kiyoshi Matsuo,¹ Shunsuke Yuzuriha,¹ Huimin Yan² and Jun Nakayama²

Departments of ¹Plastic and Reconstructive Surgery, ²Molecular Pathology, Shinshu University Graduate School of Medicine, Matsumoto, Japan

(Received December 23, 2009/Revised February 17, 2010/Accepted February 21, 2010/Accepted manuscript online February 27, 2010/Article first published online March 25, 2010)

As infrared penetrates the skin, thermal effects of infrared irradiation on cancer cells have been investigated in the field of hyperthermia. We evaluated non-thermal effects of infrared irradiation using a specialized device (1100–1800 nm with filtering of wavelengths between 1400 and 1500 nm and contact cooling) on cancer cells. In *in vitro* study, five kinds of cultured cancer cell lines (MCF7 breast cancer, HeLa uterine cervical cancer, NUGC-4 gastric cancer, B16F0 melanoma, and MDA-MB435 melanoma) were irradiated using the infrared device, and then the cell proliferation activity was evaluated by 3-(4,5-dimethylthiazol-2-yl)-5-(3-carboxymethoxyphenyl)-2-(4-sulfophenyl)-2H-tetrazolium (MTS) assay. Proliferation of all the cancer cell lines was significantly suppressed by infrared irradiation. Total infrared output appeared to be correlated with cell survival. Increased temperature during infrared irradiation appeared not to play a role in cell survival. The maximum temperature elevation in the wells after each shot in the 20 and 40 J/cm² culture was 3.8°C and 6.9°C, respectively. In addition, we have shown that infrared irradiation significantly inhibited the tumor growth of MCF7 breast cancer transplanted in severe combined immunodeficiency mice and MDA-MB435 melanoma transplanted in nude mice *in vivo*. Significant differences between control and irradiated groups were observed in tumor volume and frequencies of TUNEL-positive and Ki-67-positive cells. These results indicate that infrared, independent of thermal energy, can induce cell killing of cancer cells. As this infrared irradiation schedule reduces discomfort and side effects, reaches the deep subcutaneous tissues, and facilitates repeated irradiations, it may have potential as an application for treating various forms of cancer. (*Cancer Sci* 2010; 101: 1396–1402)

Photodynamic therapy (PDT) is the most common antitumor therapy using infrared (IR) light for select forms of cancer.⁽¹⁾ Photodynamic therapy is based on the accumulation of a photosensitizing agent in tumors and uses wavelengths near 800 nm as a photoactivating wavelength to achieve maximum penetration depth.⁽²⁾ This wavelength, however, also has high melanin absorption limiting the ability to deliver light to highly pigmented tumors.⁽³⁾ While wavelengths near 800 nm are the standard activators for PDT, other wavelengths have shown treatment promise. Santana *et al.* reported that near-IR light at 904 nm may have antitumor activity and increases cytomorphological changes with apoptosis in neoplastic cells.⁽⁴⁾ Additionally, actively proliferating cells show increased sensitivity to red and near-IR light.^(5,6) Infrared irradiation alone appears to induce DNA strand breaks and cell death by apoptosis,⁽⁷⁾ eliciting photodisruptive destruction of tumor tissue.⁽⁸⁾ While IR irradiation appears to damage tumor tissue, it is also shown to reduce cellular protein damage produced by biological oxidants in normal cells.⁽⁹⁾

Many different IR devices and lasers are used in antitumor therapies such as PDT and hyperthermia, typically utilizing wavelengths between 750 to 3000 nm. Wavelength selection directly influences target selection and penetration depth. Wave-

lengths below 1100 nm are absorbed preferentially by melanin in the superficial layers of skin (Fig. 1a). Wavelengths between 1400 to 1500 nm and above 1850 nm are absorbed heavily by water, resulting in heating to the superficial layers of the skin. To deliver IR energy safely to deeper tissues without significant superficial heating requires wavelengths between 1100 nm and 1850 nm excluding the range from 1400–1500 nm.⁽¹⁰⁾

Although many studies have elucidated the influences of IR irradiation, no studies have investigated the effects of IR irradiation using a specialized broad spectrum light source emitting light from 1100–1800 nm (with a filter to exclude wavelengths between 1400 and 1500 nm) on cancer cells. We hypothesized that this specialized IR irradiation source may kill cancer cells and have beneficial uses for cancer treatment. To investigate the potential effects of this IR irradiation for cancer treatment, we performed both *ex vivo* and *in vivo* testing. 3-(4,5-Dimethylthiazol-2-yl)-5-(3-carboxymethoxyphenyl)-2-(4-sulfophenyl)-2H-tetrazolium (MTS) assay was used to investigate the effects on various kinds of cultured cancer cells. *In vivo* studies examined pathology of implanted cancer cells in severe combined immunodeficiency (SCID) mice and nude mice.

Materials and Methods

Infrared device. Infrared irradiation was performed with a broadband IR source (Titan; Cutera, Brisbane, CA, USA). The IR device emits a spectrum of IR between 1100 to 1800 nm, with water filtering to remove wavelengths between 1400 and 1500 nm. This delivers IR without the wavelengths that are strongly absorbed by water and hemoglobin (Fig. 1b), allowing for safe delivery of IR energy deeper into tissue. The system delivers energy with a fluence range of from 5 to 56 J/cm² using continuous energy single irradiation pulses of 4 to 10 s. The IR dosimetry was performed by laser measurement instrumentation (L40(150)A-SH-V1) purchased from Ophir (North Logan, UT, USA). The sapphire contact cooling tip is set to a fixed temperature of 20°C to provide contact cooling. Pre-, parallel-, and post-cooling of the superficial layers accomplished through this temperature-controlled sapphire window further prevents excessive superficial heating.

Cell culture. Testing was conducted on cultures of five cancer cell lines: MCF7 breast cancer cells, HeLa uterine cervical cancer cells, NUGC-4 gastric cancer cells, B16F0 melanoma cells, and MDA-MB435 melanoma cells. MCF7 breast cancer cells, HeLa uterine cervical cancer cells, B16F0 melanoma cells, and MDA-MB435 melanoma cells were obtained from the American Type Culture Collection (Manassas, VA, USA), and NUGC-4 gastric cancer cells were obtained from Riken BRC Cell Bank (Ibaraki, Japan). MCF7, HeLa B16F0, and MDA-MB435 cells were maintained in DMEM (Invitrogen, Carlsbad, CA, USA), and NUGC-4 in RPMI-1640 (Invitrogen) medium supplemented with 10% fetal bovine serum and antibiotics. Cells were seeded

³To whom correspondence should be addressed. E-mail: yoheit@shinshu-u.ac.jp

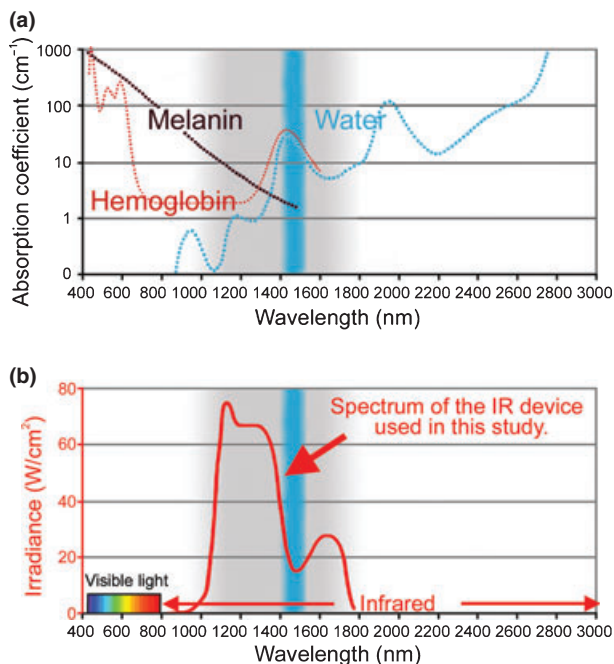


Fig. 1. (a) The absorption coefficients of melanin (brown), hemoglobin (red), and water (blue). (b) The infrared (IR) device used in the present study emits a spectrum of IR from 1100 to 1800 nm (bold red), with filtering of wavelengths between 1400 and 1500 nm (blue belt), which are strongly absorbed by water and hemoglobin. This specialized spectrum with the water filter and contact cooling system prevent pain and epidermal burns.

in 96-well microtiter plates at a concentration of 5×10^3 cells per well in 100 μL of medium. All cells were grown at 37°C in a humidified incubator with 5% CO_2 . A total of 726 wells of cancer cell lines were prepared for this study.

Cell culture and IR irradiation. Cancer cells from all five cultures were divided based on the number of individual IR exposures in a single session, and the total irradiation received. The numbers of shots performed per round were 3, 10, and 20 shots, using two separate fluence settings per shot of 20 and 40 J/cm^2 , because our preliminary results indicated that three shots at 10 J/cm^2 on cultured cancer cells (NUGC-4 cells and B16F0 cells) was not effective. This resulted in seven different groups (including the control group) within each of the five cancer cell lines. The irradiated groups were exposed to a single round of irradiation. The MTS assay was performed after a 3-day incubation period following the exposure session.

Well temperature measurement. Well temperatures were monitored during exposure sessions and sequential pulses were only delivered after well temperature returned to 37°C. This was monitored to prevent accumulated heating from multiple exposures from impacting the data. The temperatures of cultured media in the wells were monitored at 4-mm depth using a digital thermometer MC3000-000 with a sheathed thermocouple (IHKN053; 0.3 mm outer diameter of sheathed temperature sensor) purchased from Chino (Tokyo, Japan). The temperatures were recorded by 2-s sampling, and five representative data were averaged to obtain a final score.

Cell proliferation assay. We performed an MTS cell proliferation assay to evaluate the effects of IR irradiation. Cell proliferation was analyzed using a CellTiter 96 Aqueous Cell Proliferation Assay kit (Promega, Madison, WI, USA). Aliquots of 20 μL of MTS reagent were added to the wells and incubated at 37°C in a humidified incubator for 2 h. Absorbance at 490 nm (OD_{490}) was monitored with a Powerscan HT microplate reader (Dainippon Pharmaceutical, Osaka, Japan).

In vivo tumorigenicity and treatment. *In vivo* testing was conducted on two groups of mice, SCID mice and nude mice. Animals were housed in a temperature-controlled environment under a 12-h light–dark cycle with free access to water and standard mouse chow. Body weight and tumor size were measured every other day. Tumor volumes were defined as $4/3 \times \pi \times (\text{longest diameter})/2 \times (\text{shortest diameter})/2 \times (\text{shortest diameter})/2$. This study was approved by the Institutional Review Board for Animal Study of Shinshu University. National and international principles of laboratory animal care were followed throughout this study. Fourteen female SCID mice (CB17/Icr-Prkdcscid/CrlCrIj) were obtained from Charles River Laboratories (Yokohama, Japan). MCF7 cells (2.5×10^6 cell/100 μL /mouse) were implanted subcutaneously in the right flank of 6-week-old SCID mice. Ten mice were divided into two groups once tumor volume expanded to approximately 60 mm^3 . This occurred 9 days after cancer transplantation, and was defined as Day 1 for testing. Groups consisted of two equal groups ($n = 5$ for each group); one group (control group) was untreated, whereas the other group was treated by IR irradiation. Infrared irradiation was started on Day 1, and seven rounds were performed. These rounds of IR irradiation were performed every other day. One round consisted of 10 shots of IR irradiation at 20 J/cm^2 . Animals were euthanized at 46 days after cancer transplantation (Day 37).

In parallel, 40 female nude mice (Crlj;CD1-Foxn1nu) were obtained from Charles River Laboratories. MDA-MB435 cells (5.0×10^6 cell/100 μL /mouse) were implanted subcutaneously in the right flank of 6-week-old SCID mice. Twenty-eight mice were divided into two groups when tumor volume expanded to approximately 100 mm^3 . This occurred 19 days after cancer transplantation, and was defined as Day 1 for testing. Groups consisted of two equal groups ($n = 14$ for each group); one group (control group) was untreated, whereas the other group was treated by IR irradiation. Infrared irradiation was started on Days 1 and 31. Treatments were performed once daily for 13 days. All treatments consisted of 10 exposures of IR irradiation at 40 J/cm^2 . Animals were euthanized at 99 days after cancer transplantation (Day 80).

Histological investigation. MCF7 tumors were taken from the SCID mice on Days 13 ($n = 2$) and 37 ($n = 8$), and MDA-MB435 tumors were taken from nude mice on Days 3 ($n = 4$), 9 ($n = 4$), and 45 ($n = 4$), and Day 80 ($n = 16$) for histological examination. Specimens were fixed in 20% neutral buffered formalin and processed for paraffin embedding. MCF7 tumors were then serially sectioned on the horizontal plane and MDA-MB435 tumors were serially sectioned on the vertical plane (3- to 4- μm thickness). Specimens were evaluated by hematoxylin–eosin staining, transferase-mediated dUTP nick-end labeling (TUNEL) technique, and immunohistological staining using Ki-67. Frequencies of TUNEL-positive cells and Ki-67-positive cells were evaluated using digital photographs. Images were scanned and quantified in five representative fields per section, then averaged to obtain a final score. The sections were photographed under an Olympus BX51 microscope (Olympus, Tokyo, Japan) equipped with a digital camera system (DP50; Olympus). The digital photographs were processed with Adobe Photoshop (Adobe, San Jose, CA, USA).

Statistical analyses. The differences between groups at each time point were examined for statistical significance with the Student's *t*-test. $P < 0.05$ was considered to indicate statistical significance.

Results

Cell viability measured by MTS assay. The OD_{490} values of irradiated cell cultures decreased significantly compared with controls in all cultures except at the lowest dose of irradiation at

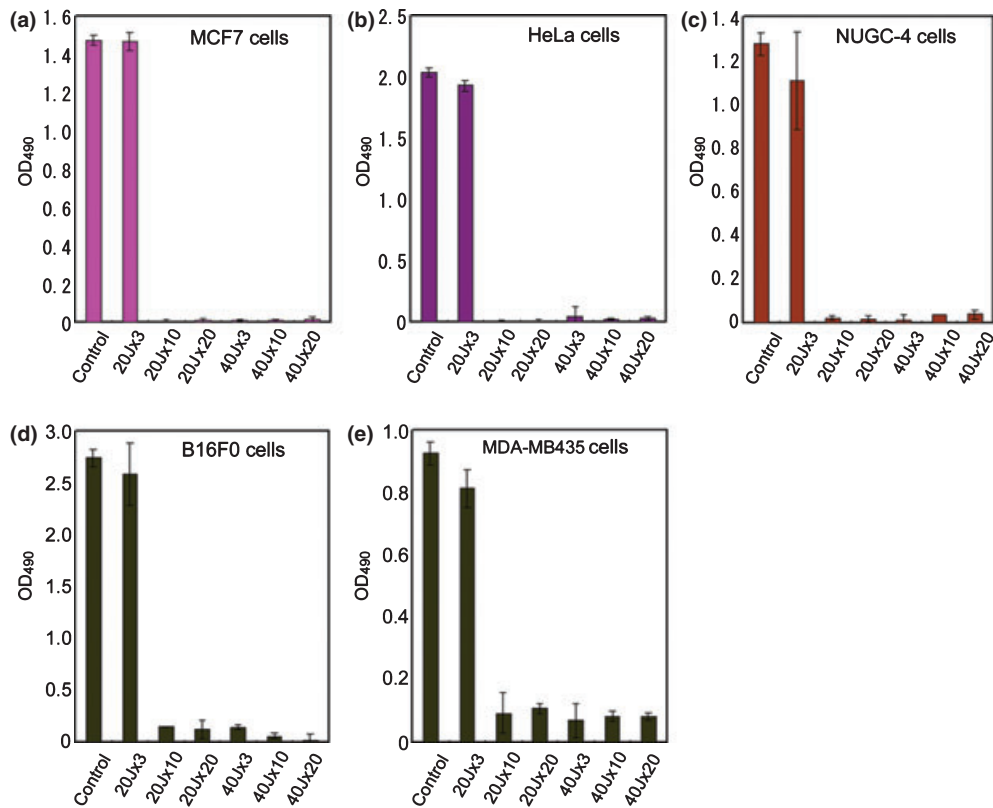


Fig. 2. OD₄₉₀ values in MCF7 breast cancer cells (a), HeLa uterine cervical cancer cells (b), NUGC-4 gastric cancer cells (c), B16F0 melanoma cells (d), and MDA-MB435 melanoma cells (e). The OD₄₉₀ values of irradiated cell cultures excluding the lowest irradiation group of three shots at 20 J/cm² decreased significantly ($P < 0.001$, compared with controls) in all cultures.

20 J/cm² for three exposures (group 20 J × 3; $P < 0.001$; Fig. 2). Group 20 J × 3 showed the smallest decrease with significant reductions in HeLa cells ($P = 0.040$) and MDA-MB435 cells ($P = 0.034$), but only modest reductions were observed in MCF7, NUGC-4, and B16F0 cells. No statistically significant intra-group differences were observed between the 20 and 40 J/cm² groups (excluding group 20 J × 3). This was consistently observed for all cancer cell lines.

Well temperatures. In order to exclude the possibility of thermal damage to cancer cells, well temperatures were recorded at the bottom of the culture well (4 mm) by 2-s sampling. Temperature rise during each 20 J/cm² shot was $3.76 \pm 0.53^\circ\text{C}$, rising from 37°C to $40.76 \pm 0.53^\circ\text{C}$ during IR irradiation. Temperature returned to baseline (37°C) 43.8 ± 3.58 s later. The period over 40°C was 3.6 ± 2.63 s during each 20 J/cm² shot. Temperature rise during a 40 J/cm² exposure was $6.85 \pm 0.58^\circ\text{C}$; rising from 37°C to $43.85 \pm 0.58^\circ\text{C}$ required 83.4 ± 8.11 s to return to baseline temperature. The period over 40°C was 42.1 ± 4.07 s during each 40 J/cm² shot (Fig. 3a,b).

Clinical findings during IR irradiation. Infrared irradiation induced no pain, and mice did not withdraw even though IR irradiation was performed without anesthesia. No side effects, such as epidermal burns, were observed during the study.

Effect of IR irradiation on tumors transplanted to mice. The mean tumor volume of MCF7 in the control group was 62.0 ± 2.4 mm³ on Day 1 of the treatment, increased rapidly from through Day 7, and ended up at 120.6 ± 15.6 mm³ on Day 37. In the irradiated MCF7 group, tumor volume was 69.6 ± 4.7 mm³ on Day 1 of the treatment and decreased after the first round of IR irradiation. Mean tumor volume decreased

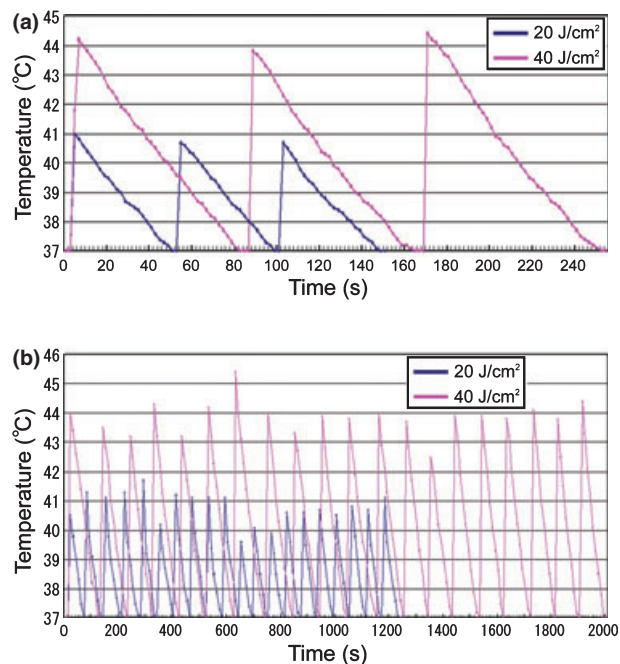


Fig. 3. The well temperatures irradiated 3 (a) and 20 (b) shots at 20 J/cm² (blue) and 40 J/cm² (red). The temperatures of cultured media were monitored at 4-mm depth in wells during exposure sessions and sequential pulses were only delivered after the well temperature returned to 37°C.

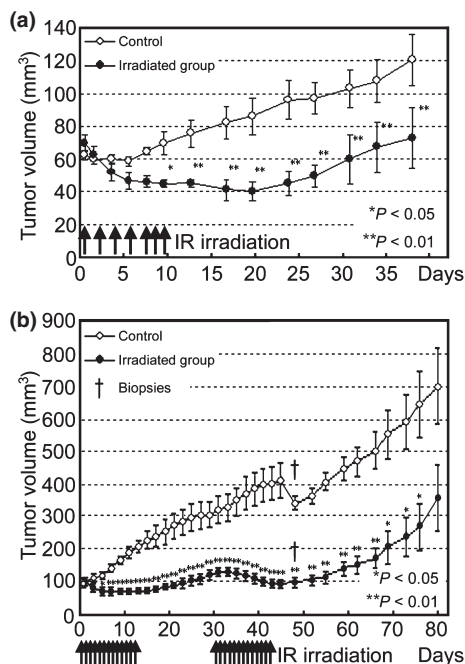


Fig. 4. Relative tumor volume in MCF7 (a) and MDA-MB435 (b) cells. Significant differences were observed in MCF7 tumor volume between the control and infrared (IR)-irradiated group from Days 9 through 37, when the animals were euthanized. Significant differences were observed in MDA-MB435 tumor volume between the control and IR-irradiated groups from Day 5 up to Day 77. Significant differences are indicated (* $P < 0.05$, ** $P < 0.01$). Cross sign indicates when two animals of each group were euthanized for histological investigation (Day 45).

steadily through Day 19 with a minimum volume of $40.2 \pm 5.7 \text{ mm}^3$. Mean tumor volume began to increase gradually in irradiated group after Day 20 ending at $72.9 \pm 18.4 \text{ mm}^3$

on Day 37. Tumor volume differences were statistically significant between the control and IR-irradiated groups from Day 9 when the fifth round of IR irradiation was performed through Day 37 when the animals were euthanized (Fig. 4a).

The mean tumor volume of MDA-MB435 in the control group was $99.0 \pm 26.85 \text{ mm}^3$ on Day 1 of the treatment and increased continuously to $700.5 \pm 333.8 \text{ mm}^3$ on Day 80. The mean tumor volume for the irradiated MDA-MB435 group was $100.0 \pm 26.06 \text{ mm}^3$ on Day 1 of the treatment. Tumor volume decreased after the first round of IR irradiation and continued to reduce through Day 5 with a minimum volume of $67.0 \pm 15.75 \text{ mm}^3$. After Day 5, the mean tumor volume gradually increased in the irradiated group through Day 15, resulting in $129.0 \pm 44.05 \text{ mm}^3$ on Day 31 when the second treatment started. Following the second round of irradiation, the mean tumor volume again decreased, reducing to $94.0 \pm 41.22 \text{ mm}^3$ by Day 45. The mean tumor volume began to increase gradually and ended up at $357.3 \pm 297.2 \text{ mm}^3$ (Day 80). Significant differences were observed in tumor volume between the control and IR-irradiated groups from Day 5 up to Day 77 (Fig. 4b).

Histological analysis of tumor after IR irradiation. The histology of irradiated groups showed tumor shrinkage in MCF7 and MDA-MB435 cells (Figs 5,6). Injured cells were observed in the center of the tumors, in particular in MCF7 on Day 37 and MDA-MB435 on Day 45 (Figs 5b,6b).

In the MCF7 group, frequencies of TUNEL-positive cells in the irradiated group were high on Days 13 and 37, compared to the control group. Frequencies of Ki-67-positive cells in the irradiated group were low on Days 13 and 37, compared to the control group (Fig. 7a). Significant differences were observed between the control and IR-irradiated groups in all four groups ($P < 0.05$). Frequencies of TUNEL-positive cells in the control and irradiated groups on Day 13 were $2.30 \pm 0.84\%$ and $19.33 \pm 5.05\%$, respectively. Frequencies of TUNEL-positive cells in the control and irradiated groups on Day 37 were $3.15 \pm 0.71\%$ and $6.63 \pm 1.29\%$, respectively. Frequencies of Ki-67-positive cells in the control and irradiated groups on Day

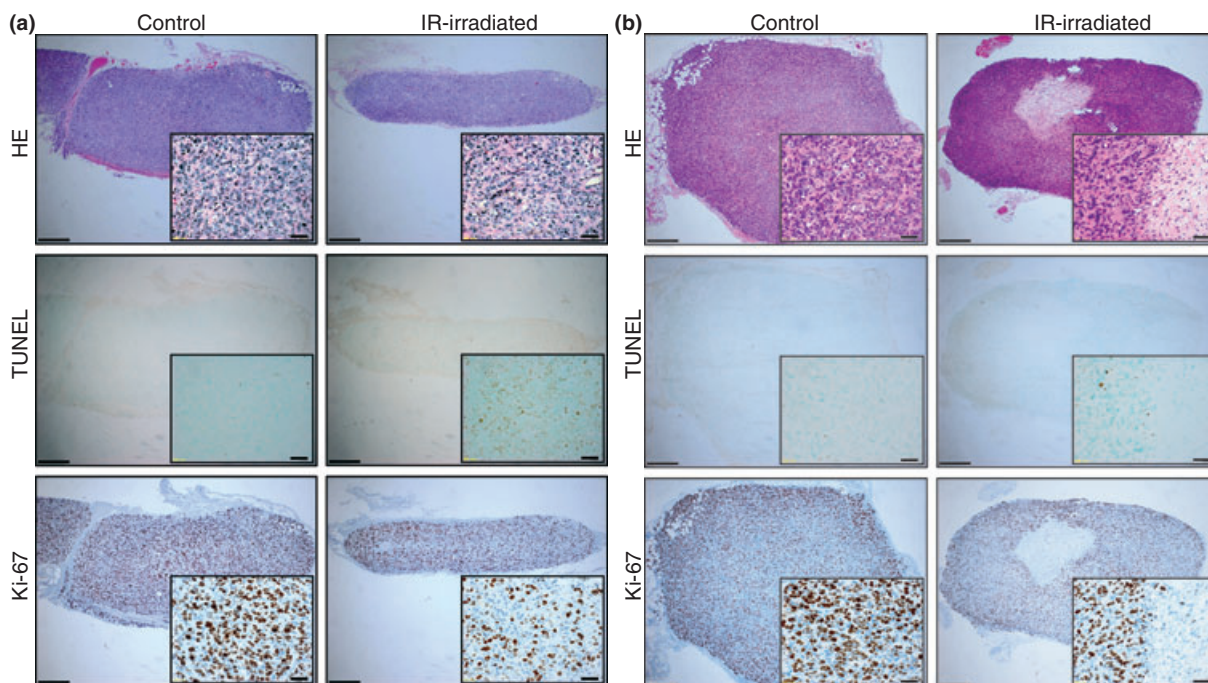


Fig. 5. The horizontal sectional histology of control and infrared (IR)-irradiated MCF7 breast cancer cells on Days 13 (a) and 37 (b). The left column shows control tissues, and the right column shows IR-irradiated tissues. Images from top to bottom show hematoxylin-eosin staining, TUNEL technique, and immunohistochemical staining using Ki-67. Scale bars = $400 \mu\text{m}$ (magnification: $\times 40$). Insets: scale bars = $40 \mu\text{m}$ (magnification: $\times 400$).

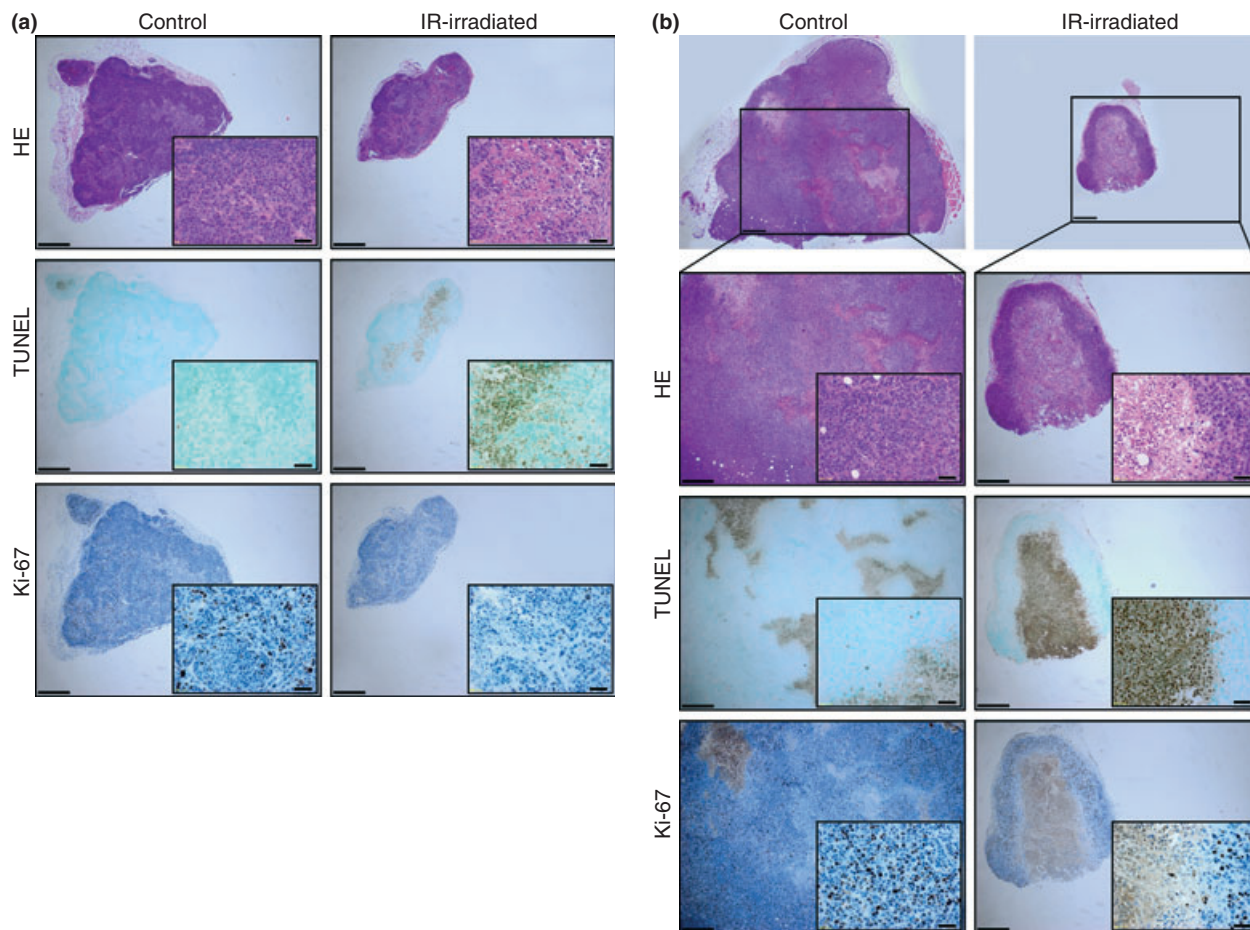


Fig. 6. The vertical sectional histology of control and infrared (IR)-irradiated MDA-MB435 melanoma cells on Days 9 (a) and 45 (b). The left column shows control tissues, and the right column shows IR-irradiated tissues. Images from top to bottom show hematoxylin–eosin staining, TUNEL technique, and immunohistological staining using Ki-67. Scale bars = 400 μm (magnification: $\times 40$). Insets: scale bars = 40 μm (magnification: $\times 400$).

13 were $72.10 \pm 6.40\%$ and $40.1 \pm 5.26\%$, respectively, and $57.40 \pm 11.73\%$ and $42.12 \pm 5.40\%$, respectively, on Day 37.

Similarly, in the MDA-MB435 group, frequencies of TUNEL-positive cells in the irradiated group were high on Days 9 and 45, compared to the control group. Frequencies of Ki-67-positive cells in the irradiated group were low on Days 9 and 45, compared to the control group (Fig. 7b). Significant differences were observed between the control and IR-irradiated groups (both in the center and the superficial layer of tumor) in all four groups ($P < 0.05$). Frequencies of TUNEL-positive cells in the control and irradiated groups were $0.84 \pm 0.47\%$ and $15.86 \pm 11.18\%$, respectively, on Day 9. Frequencies of TUNEL-positive cells on Day 45 in the control group, in the superficial layer of the irradiated tumor, and in the center of the irradiated tumor, were $1.09 \pm 0.44\%$, $6.68 \pm 4.17\%$, and $78.12 \pm 4.93\%$, respectively. Frequencies of Ki-67-positive cells in the control and irradiated groups on Day 9 were $11.42 \pm 6.45\%$ and $0.76 \pm 0.12\%$, respectively. Frequencies of Ki-67-positive cells on Day 45 in the control group, in the superficial layer of the irradiated tumor, and in the center of the irradiated tumor, were $21.06 \pm 5.47\%$, $8.04 \pm 3.762\%$, and $1.21 \pm 1.29\%$, respectively.

Discussion

This study demonstrates that using a specific wavelength of IR (1100–1800 nm with filtering of wavelengths between 1400 and 1500 nm) suppresses tumor growth, independent of thermal

energy. Further, due to contact cooling, this light energy can be applied to the body externally without complications.

We previously reported that IR irradiation induces an injury response in the skin and subcutaneous tissue.^(11,12) Thermal damage, including IR irradiation, denatures the collagen and encourages the generation of new collagen, resulting in tighter skin.⁽¹³⁾ Non-ablative lasers work by thermally stimulating dermal collagen remodeling.⁽¹⁴⁾ To protect the subcutaneous tissues against IR, hemoglobin and fluid absorb IR through blood vessel dilation and the skin turning red or foam formation.⁽¹²⁾ This is because IR is strongly absorbed by hemoglobin and fluids.⁽¹²⁾ Thus, the dermis tends to increase the amount of fluid by inducing increases in collagen, elastin, and water-binding protein to protect the subcutaneous tissues against IR.^(11,12) These increases in the amount of fluid may indicate an attempt by the body to further reduce the level of future IR penetration to deeper tissue structures.^(11,12)

Infrared irradiation can penetrate deep into subcutaneous human tissue (up to 12 mm), where it can cause photochemical changes.^(15–17) The penetrating 600–1300 nm wavelength region causes photochemical changes and affects a large volume and depth of tissue.⁽¹⁸⁾ In a study using near-IR irradiation at 904 nm, irradiation was shown to increase cytomorphologic changes with programmed cellular death in neoplastic cells; however, no apparent changes were observed in non-neoplastic cells.⁽⁴⁾ Unlike wavelengths beyond 1100 nm where melanin absorption is negligible,⁽¹⁸⁾ absorption at 904 nm is significant.

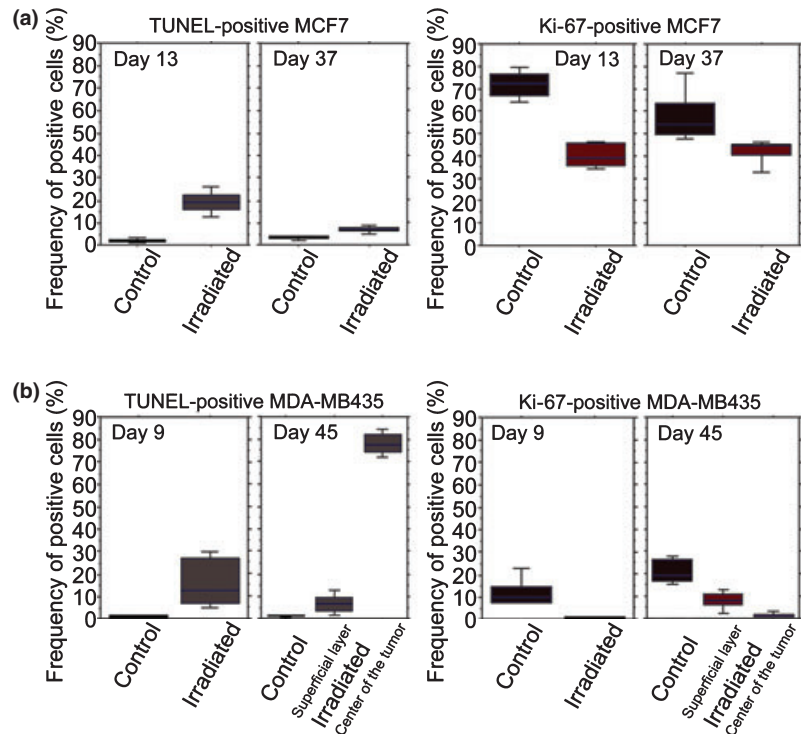


Fig. 7. Mean scores of frequencies of TUNEL-positive cells and Ki-67-positive cells. MCF7 (a) and MDA-MB435 (b). Significant differences were observed between the control and infrared (IR)-irradiated groups in all four groups ($P < 0.05$).

This may limit possible uses of the 904 nm wavelength for certain body areas in races with skin rich in melanin.

To deliver light energy or IR safely to the deeper tissues, wavelengths below 1100 nm, from 1400 to 1500 nm and above 1850 nm, need to be filtered out of the delivered spectrum. Without filtering, too much energy is absorbed in the superficial layers of skin, limiting safe energy delivery to deeper tissue. In this study, we used an IR device that emits a spectrum of IR from 1100 to 1800 nm, with filtering of wavelengths between 1400 and 1500 nm that are strongly absorbed by fluid and hemoglobin (Fig. 1b). Internal to the device, a water filter absorbs high water absorption IR wavelengths preventing emission of wavelengths that would lead to superficial heating, which can lead to painful sensations and burns.⁽¹⁷⁾ This IR device cools the superficial layers through a temperature-controlled sapphire window to prevent the surface temperature from increasing severely during irradiation.⁽¹³⁾ This specific wavelength and cooling system enable IR to penetrate to deeper tissues without any pain or epidermal burns. This was evidenced by the ability to treat mice without anesthesia and without contact burns or other adverse events.

Irradiated cell cultures showed significant decreases in cell counts in all cultures except at the lowest dose of irradiation in group 20 J × 3. Correlation to efficacy seemed to be highest with total delivered energy, not per pulse fluence, as lower output, multiple irradiations appeared as equally effective as higher fluence irradiations. Ten shots at 20 J/cm² achieved a comparable significant reduction in cell count to three shots at 40 J/cm². Three shots at 20 J/cm² appeared close to a threshold energy dosage. Further studies are required to determine the accurate correlations between irradiation dose and cell survival, and the different effects in each cancer cell line.

We have shown that IR irradiation significantly inhibited the tumor growth of MCF7 in SCID mice and MDA-MB435 in nude mice at the *in vivo* level. Significant differences were observed in tumor volume and frequency of TUNEL-positive and Ki-67-positive cells between the control and IR-irradiated groups. The histology of irradiated groups showed tumor shrinkage and injured cells in the center of tumor. Contact cooling (20°C) by

this IR device allowed IR to penetrate deeper tissues, thus inducing central tumor injury. The frequency of TUNEL-positive cells in the irradiated group was significantly higher than in the control group for both MCF7 and MDA-MB435, which supports the notion that IR irradiation induces apoptosis of cancer cells. The frequency of Ki-67-positive cells in the irradiated group was significantly lower than in the control group for both MCF7 and MDA-MB435, which suggests that IR irradiation could suppress proliferation of cancer cells.

Infrared typically induces molecular vibrations^(16,19) and rotations causing an increase in temperature. However, in *in vivo* studies, IR penetrates the skin and reaches the subcutaneous tissue without a significant increase in skin temperature.⁽¹⁶⁾ The effects of IR are independent of generated heat.⁽²⁰⁾ In the present study, increased temperature appeared not to play a role in cell culture survival rate. Results in the 20 J/cm² group (excluding group 20 J × 3) were statistically equivalent to the 40 J/cm² group and the maximum temperature rise during exposure in the 20 J/cm² group was only 3.76°C (temperature = 40.76°C). This is roughly equivalent to a fever induced by a bad illness. Further, elevated temperatures only remained above 40°C for 3.6 s, far short of damage observed during prolonged high grade fevers. The rationale of hyperthermia is based on a direct cell-killing effect at temperatures above 41–42°C.⁽²¹⁾ With whole-body hyperthermia, tumor growth suppression requires temperatures of about 42°C with exposure of at least 60 min.⁽²²⁾ Even though the extent and duration of temperature elevation were not significant in relation to the cases of hyperthermia, irradiated cell cultures showed significant decreases in cell counts in the present study. This level of temperature rise is not associated with tumor growth suppression indicating that a factor other than hyperthermia is responsible for growth suppression of the cancer cell lines.

In the present study, even very low output and fewer shots of IR (10 IR shots at 20 and 40 J/cm²) inhibited tumor growth. This output is so low that in human skin even the sensation of heat will not be felt due to contact cooling. This IR irradiation induced no pain, and mice did not withdraw even though IR treatment was performed without anesthesia. Further, side

effects such as epidermal burns were not observed, and mice looked healthy throughout of the study. Further studies are necessary to determine if more output, increased frequency of treatments, and/or longer periods of irradiation may be even more effective in suppressing tumor growth.

The advantages of this IR irradiation schedule are the reduction discomfort and side effects, and low cost. Taken together, these characteristics facilitate repeated irradiations, which if proven beneficial for cancer cell reduction in humans, may provide an alternative or adjunct treatment for patients, offering improved results and/or patient quality-of-life. This IR irradiation is frequently performed for other indications at a level of 40 J/cm², with a very high safety record and no significant complications.^(1,3)

It should be noted that this was a preliminary study based on experiments in a limited variety of cancer cell lines. Further

studies are warranted in larger numbers and various types of cancer cells and with longer post-treatment periods to evaluate variations in treatment parameters and correlations with other antitumor therapies. These studies promise to contribute to the design of more efficacious cancer treatments.

Acknowledgments

We thank the members of Cutera Inc. for technical information relative to the infrared device and helpful comments. This work was supported in part by a Grant-in-Aid for Scientific Research (no. 21390104 to J. N.) from the Japan Society for the Promotion of Science.

Disclosure Statement

The authors have no conflict of interest.

References

- 1 Dougherty TJ, Gomer CJ, Henderson BW *et al*. Photodynamic therapy. *J Natl Cancer Inst* 1998; **90**: 889–905.
- 2 Lobel J, MacDonald IJ, Ciesielski MJ *et al*. 2-(1-hexyloxyethyl)-2-devinylpyropheophorbide-a (HPPH) in a nude rat glioma model: implications for photodynamic therapy. *Lasers Surg Med* 2001; **29**: 397–405.
- 3 Busetti A, Soncin M, Jori G, Kenney ME, Rodgers MA. Treatment of malignant melanoma by high-peak-power 1064 nm irradiation followed by photodynamic therapy. *Photochem Photobiol* 1998; **68**: 377–81.
- 4 Santana-Blank LA, Rodriguez-Santana E, Vargas F *et al*. Phase I trial of an infrared pulsed laser device in patients with advanced neoplasias. *Clin Cancer Res* 2002; **8**: 3082–91.
- 5 Karu T, Pyatibrat L, Kalendo G. Irradiation with He-Ne laser can influence the cytotoxic response of HeLa cells to ionizing radiation. *Int J Radiat Biol* 1994; **65**: 691–7.
- 6 Tafur J, Mills PJ. Low-intensity light therapy: exploring the role of redox mechanisms. *Photomed Laser Surg* 2008; **26**: 321–6.
- 7 Tirlapur UK, König K. Femtosecond near-infrared laser pulse induced strand breaks in mammalian cells. *Cell Mol Biol* 2001; **47**: 131–4.
- 8 Dees C, Harkins J, Petersen MG, Fisher WG, Wachter EA. Treatment of murine cutaneous melanoma with near infrared light. *Photochem Photobiol* 2002; **75**: 296–301.
- 9 Kujawa J, Zavodnik IB, Lapshina A, Labieniec M, Bryszewska M. Cell survival, DNA, and protein damage in B14 cells under low-intensity near-infrared (810nm) laser irradiation. *Photomed Laser Surg* 2004; **22**: 504–8.
- 10 Davenport SA, Gollnick DA, Levernier M, Spooner GJR. Method and system for treatment of post-partum abdominal skin redundancy or laxity. United States Patent 20060052847. Available from URL: <http://www.freepatentsonline.com/y2006/0052847.html>
- 11 Tanaka Y, Matsuo K, Yuzuriha S, Shinohara H. Differential long-term stimulation of type I versus type III collagen after infrared irradiation. *Dermatol Surg* 2009; **35**: 1099–104.
- 12 Tanaka Y, Matsuo K, Yuzuriha S. Long-term evaluation of collagen and elastin following infrared (1100 to 1800 nm) irradiation. *J Drugs Dermatol* 2009; **8**: 708–12.
- 13 Goldberg DJ, Hussain M, Fazeli A, Berlin AL. Treatment of skin laxity of the lower face and neck in older individuals with a broadspectrum infrared light device. *J Cosmetic Laser Ther* 2007; **9**: 35–40.
- 14 Lipper GM, Perez M. Nonabrasive acne scar reduction after a series of treatments with a short-pulsed 1064-nm neodymium: YAG laser. *Dermatol Surg* 2006; **32**: 998–1006.
- 15 Karu T. Invited review. Primary and secondary mechanisms of action of visible to near-IR radiation on cells. *J Photochem Photobiol B: Biol* 1999; **49**: 1–17.
- 16 Schieke SM, Schroeder P, Krutmann J. Review article. Cutaneous effects of infrared radiation: from clinical observations to molecular response mechanisms. *Photodermatol Photoimmunol Photomed* 2003; **19**: 228–34.
- 17 Kelleher DK, Thews O, Rzeznik J, Scherz A, Salomon Y, Vaupel P. Hot topic. Water-filtered infrared-A radiation: a novel technique for localized hyperthermia in combination with bacteriochlorophyll-based photodynamic therapy. *Int J Hyperthermia* 1999; **15**: 467–74.
- 18 Anderson RR, Parrish JA. The optics of human skin. *J Invest Dermatol* 1981; **77**: 13–9.
- 19 Pujol JA, Lecha M. Photoprotection in the infrared radiation range. *Photodermatol Photoimmunol Photomed* 1993; **9**: 275–8.
- 20 Danno K, Mori N, Toda K, Kobayashi T, Utami A. Near-infrared irradiation stimulates cutaneous wound repair: laboratory experiments on possible mechanisms. *Photodermatol Photoimmunol Photomed* 2001; **17**: 261–5.
- 21 Dewey WC. Arrhenius relationships from the molecule and cell to clinic. *Int J Hyperthermia* 1994; **10**: 457–83.
- 22 Wust P, Hildebrandt B, Sreenivasa G *et al*. Review article. Hyperthermia in combined treatment of cancer. *Lancet Oncol* 2002; **3**: 487–97.